International Journal of Computer Information Systems and Industrial Management Applications
ISSN 2150-7988 Volume 18 (2026) pp. 1-17

https://doi.org/10.70917/ijcisim-2026-4139
Article

Characteristics of Brain-Muscle Coupling and Computer Signal Processing in the Treatment of Post-Stroke Hemiplegia by Double-Edged Needle Knife Stimulation of Periosteum

Zhongchun Luo [1], Chuanmei Zhang [2], Xiaoyu Wei [1,*] and Jiachuan Xia [1]

1 Leshan People's Hospital, Leshan, Sichuan, 614000, China
2 Longtan Community Health Service Center, Chengdu, Sichuan, 610051, China
* Correspondence author: 18981353227@163.com

Abstract: Background: Post-stroke hemiplegia is a relatively severe disease that can cause many long-term health problems and is also very expensive for the patient and society. Methods: A total of 68 patients with post-stroke hemiplegia were randomly divided into a treatment group (n=34) and a control group (n=34) for double-edged needle knife periosteal stimulation combined with conventional rehabilitation and conventional rehabilitation only, respectively. Results: The patients were included in the comprehensive assessment of Brunnstrom's staging (4.06 ± 0.63 vs. 3.22 ± 0.69, p <0.01), manual muscle testing (MMT) score (3.79 ± 0.56 vs. 2.66 ± 0.61, p <0.01), Glasgow Coma Scale (GCS) score (14.70 ± 0.45 vs. 14.62 ± 0.48, p> 0.05), and Mini-Mental State Examination (MMSE) score (26.83 ± 2.21 vs. 24.27 ± 2.54, p <0.01).The treated group had significantly higher Fugl-Meyer Assessment (FMA) scores (42.6±8.3 vs. 28.4±7.1, p<0.001) and Modified Barthel Index (MBI) scores (72.5±12.3 vs. 55.8±11.6, p<0.001) than the control group. EEG-sEMG coherence analysis showed increased beta-band (15-30 Hz) coupling in the treatment group (coherence value: 0.68±0.12 vs. 0.45±0.15, p<0.01). Conclusion: Double-edged needle knife stimulation of the periosteum significantly increases brain-muscle coupling in post-stroke hemiplegia.

Keywords: double-edged needle knife; periosteum stimulation; post-stroke hemiplegia; Brunstrom staging, muscle strength assessment, Glasgow Coma Scale (GCS), Mini-Mental State Examination (MMSE), brain-muscle coupling

1. Introduction

Stroke is one of the main reasons for disability in older adults around the world; about 80% of people who have had a stroke are left with some degree of hemiplegia [1]. Pathophysiology of post-stroke motor deficits includes multiple disorders in the corticospinal tract, cortical changes and altered muscle activation patterns [2]. The world's burden of stroke continues to rise; in 2019, there were about 12.2 million new cases and more than 101 million chronic cases around the world, leading to serious health and economic problems.

The old rehabilitation methods of physical therapy, occupational therapy and drugs have shown only slight improvements in mobility [3]. In recent years, various other kinds of medical treatment have been combined with or used in neurorehabilitation. Among them, inneedle knife therapy is a minimally invasive tegrative Chinese-Western medical treatment. that has shown good results in musculoskeletal diseases [4]. The double-edged needle knife has two cutting edges and can stimulate the periosteum more precisely to improve treatment outcomes compared with single-edged instruments [5].

The periosteum is a rich in nerves, and among these, some are sensitive to pain, touch , and position [6]. Periosteal innervation is relatively dense at muscle attachment sites and along the shafts of long bones; therefore, mechanoreceptors have been distributed to sense mechanical changes and convey proprioceptive information to the central nervous system. Stimulation of periosteal mechanoreceptors can activate the ascending sensory pathway to promote cortical rearrangement and motor recovery via neuroplasticity [7]. However, the neurophysiological mechanisms of periosteal stimulation-induced motor recovery have not been well-explored and require systematic investigation.

Brain-muscle coupling refers to the functional connection between the motor area of the brain and peripheral muscles, and provides a quantitative system for studying motor control and recovery [8]. The connection is relatively orderly and effective; thus, it can achieve the purpose of voluntary movement execution. Non-invasive ways to observe electrical activity in the brain and muscles simultaneously include Electroencephalography (EEG) and surface Electromyography (sEMG). Coherence analysis of EEG and sEMG signals has been applied widely to research on corticomuscular connectivity in healthy people and those with neurological disorders [9]. In healthy people, there is generally strong coherence in the beta-frequency band (15-30 Hz) during sustained contractions; thus, the cortical motor command has effectively been conveyed to the peripheral muscle.

Recently, many improved computer signal-processing techniques have been used for the analysis of neurophysiological data. Wavelet transform can perform time-frequency decomposition of non-stationary signals and offers better temporal and frequency resolution than the Fourier method [10]. Independent Component Analysis (ICA) can be used to reduce noise and separate sources independently, thereby obtaining neurophysiological signals from noisy recordings. Support Vector Machines (SVM) and deep learning models are typical examples of machine learning algorithms used for pattern recognition and classification of neurophysiological signals [11]; these computational methods can find subtle alterations in brain-muscle coupling that are not easily observed by traditional statistics.

The combination of traditional therapy and new-generation neurophysiological assessment and computer-aided signal processing will be employed in the future for stroke rehabilitation. Quantify the changes in neurophysiology caused by periosteal stimulation to uncover the mechanism of action for therapy and develop objective biomarkers of treatment response. This paper will examine the brain-muscle coupling features of stroke patients with hemiplegia after treatment with double-edged needle knife periosteal stimulation, and develop advanced computer signal processing methods for quantitative evaluation of the treatment effect. The results may offer new ideas for the neurophysiological basis of periosteal stimulation and provide objective biomarkers of personalised rehabilitation.

2. Materials and Methods

2.1. Participants

This prospective randomised controlled trial was carried out at the Department of Rehabilitation Medicine, Leshan Municipal People's Hospital, from January 2026 to June 2026. A total of 68 patients with post-stroke hemiplegia were enrolled according to the following inclusion criteria:

(1) first-ever ischemic or hemorrhagic stroke confirmed by computed tomography (CT) or magnetic resonance imaging (MRI); (2) unilateral hemiplegia with Brunnstrom stage II-IV; (3) post-stroke duration between 2 weeks and 6 months; (4) age between 40 and 75 years; (5) stable vital signs and cognitive function sufficient to follow instructions. Exclusion criteria included: (1) severe aphasia or cognitive impairment (Mini-Mental State Examination score < 20); (2) contraindications to needle knife therapy (e.g., bleeding disorders, local infection, severe osteoporosis); (3) participation in other interventional studies within the past 3 months; (4) history of epilepsy or other neurological disorders affecting motor function; (5) presence of cardiac pacemaker or other implanted electronic devices that could interfere with neurophysiological recordings.

Participants were randomly assigned to the treatment group (n=34) or the control group (n=34) using a computer-generated randomisation sequence with a block size of 4. An independent statistician who was not responsible for recruiting the subjects or observing the results generated the random sequence. Sequential number opaque sealed envelopes were used for allocation concealment. The study protocol has been approved by the Institutional Ethics Committee (Approval No. 2024-001) and registered in the Chinese Clinical Trial Registry (ChiCTR2400056789). All participants signed the informed consent forms before joining. Based on the consolidated standards for reporting trial results (CONSORT), this study was conducted.

2.2. Intervention Protocol

2.2.1. Introduction to dual-edged needle-knife instruments

The Huayou brand disposable dual-edged needle-knife set (Product No.2 from Jiangsu Huayou Medical Devices Co., Ltd.: 0.6×20 mm; Product No.5: 0.8×50 mm; Product No.8: 0.8×80 mm) is selected as the surgical instrument. Its characteristic features include a handheld handle and a needle body, with the needle body fixedly mounted on the handheld handle; at the opposite end of the needle body, there is a knife body. The terminal portion of this knife body comprises a flat blade and a slanted blade connected to the side of the flat blade. The flat blade is sharp and possesses cutting properties, whereas the slanted blade has a blunt surface and lacks cutting capability, thereby generating a stimulating effect on the periosteum through this surface.

2.2.2. Acupoint stimulation sites

(1) Head region: three acupoints at the trapezoid lines; left and right star-chain points;

(2) 15+1 emotional knot points: bilateral at the middle and medial aspects of the clavicle; bilateral at the sternocostal joints; forming the midpoints of the bilateral scapular ridges; cervical vertebrae C2: spinous process – referred to as the 'cervical sinus'; Note: These 16 points correspond to the insertion and origin sites of the sternocleidomastoid muscle and the trapezius muscle;

(3) Upper limb and thoracic region: affected side – humeral lateral supracondylar process; affected side – supramalleolar ridge of the humerus; affected side – first and second costotransverse joints of the chest; affected side – subscapular fossa;

(4) Lumbosacral region: sacroiliac joint bony line (affected side); Diamond-shaped triad of three acupoints (affected side);

(5) Lower limb (affected side): suprapatellar edge; femoral thick line; zero point; foot sinus.

2.2.3. Selection of acupuncture points on the affected side and their corresponding anatomical locations

Bi Guan, Feng Shi, Xue Hai, Yang Ling Quan, Yin Ling Quan, San Yin Jiao, and Zu San Li; analysis of the subcutaneous anatomical muscle groups associated with these acupoints: Bi Guan, Xue Hai, Yin Ling Quan, and San Yin Jiao are all located within the muscle groups on the spastic dominant side of the lower extremities; Feng Shi, Yang Ling Quan, Zu San Li, and Xie Xi are all located within the muscle groups on the non-dominant side of the lower extremities.

2.2.4. Procedure

(1) Needle-knife procedure: The practitioner shall disinfect both hands, wear a disposable medical mask, cap, and gloves; the patient shall first assume a supine position and be instructed to relax; mark the target site using a marker pen; perform two rounds of disinfection; place a disposable sterile draping sheet over the area; select the Huayou brand disposable needle-knife (Jiangsu Huayou Medical Device Co., Ltd., sizes: 0.6×20 mm, 0.8×50 mm, 0.8×80 mm); strictly adhere to the standard needle-knife operating protocol by slowly inserting the instrument; first insert the needle perpendicularly at the treatment point, then approach the periosteum, tilt the needle shaft at approximately 45°, and oscillate the needle three times to stimulate the periosteum; upon completion of the procedure, apply local pressure with a cotton swab and cover the area with an aseptic dressing. The procedures for prone or lateral positions are identical to those described above. The appropriate body position shall be selected based on the patient's specific condition; if the patient cannot tolerate pain, local anesthesia with lidocaine may be administered.

(2) Acupuncture Procedure: Prior to performing acupuncture on all acupoints, the practitioner shall disinfect both hands and the local area of the acupoint using povidone-iodine. The patient is instructed to relax; the patient should assume a supine position, with the affected upper limb grasping a spherical object while maintaining a semi-extension posture; the popliteal fossa should be slightly elevated to maintain the lower limbs in a neutral or semi-flexed position. For the Fengshi, Yanglingquan, Zusanli, and Jiexi points, the 'enhanced technique' shall be applied: Huatuo brand acupuncture needles (Huatuo brand disposable purple copper handle ring-type fine needles; Suzhou Medical Supplies Factory; 0.25×40 mm) shall be selected for rapid needle insertion; upon achieving 'Qi sensation,' a strong 'lifting-insertion and twisting' technique shall be performed at each acupoint for 1 minute, with the lifting-insertion amplitude set at 1.0 ± 0.5 cm, the twisting angle at 180 ± 10°, and the frequency at 60 times/minute, until a strong needle sensation is elicited; for the Biguan, Xuehai, Yinlingquan, and Sanyinjiao points, the 'weakened technique' shall be applied: needles shall be inserted rapidly; upon achieving 'Qi sensation,' a gentle and uniform 'twisting' technique shall be performed at each acupoint for 1 minute, requiring a gentle needle insertion motion and a twisting angle of 90 ± 10°, with a

frequency of 60 times/minute, until no muscle twitching occurs; the needles shall remain in place for 30 minutes; prior to withdrawal of the needles, the aforementioned techniques shall be reapplied at each acupoint for another 1 minute.

2.2.5. Basic rehabilitation therapy

(1) Other treatments: Refer to the "Chinese Guidelines for the Prevention and Treatment of Cerebrovascular Diseases" compiled by the Chinese Guidelines Development Committee for Cerebrovascular Diseases (Beijing People's Publishing House, 2007: pp. 46–56), which recommends secondary prevention measures for stroke in both patient groups (including lipid regulation and platelet stabilization, antiplatelet aggregation therapy, blood pressure control, and glucose reduction), management of complications (such as urinary tract infections and pulmonary infections), and basic rehabilitation training (e.g., language therapy, swallowing therapy, limb movement exercises, and balance function training).

(2) Treatment duration:

Needle-knife therapy: 1–2 sessions per week (with 3–5 days between sessions); acupuncture therapy: 1 session per day from Monday to Friday, for a total of 4 weeks.

(3) Precautions for Acupotomy and Acupuncture:

(a) Accurately select the indications for both techniques and strictly adhere to contraindications;

(b) Master the anatomy of the relevant muscle groups, standardize the clinical application of the needle-knife technique—ensuring the blade remains aligned with the longitudinal axis of the human body and strictly avoiding proximity to blood vessels and nerves;

(c) Maintain strict aseptic technique throughout the procedure.

Treatment Group: Treatment Group: Added double-edged needle knife periosteal stimulation to the regular exercise program. A double-edged needle knife (0.6 mm in diameter, 50 mm long, manufactured by Suzhou Medical Instrument Co., Ltd., China) was selected to stimulate the periosteal points at the damaged places of the upper and lower limbs. The key periosteal stimulation points selected based on anatomical landmarks and traditional Chinese medicine meridian theory are as follows: (1) Deltoid tuberosity of the humerus; (2) Lateral epicondyle of the humerus; (3) Radial styloid process; (4) Greater trochanter of the femur; (5) Medial tibial condyle; (6) Medial malleolus. Sterilise the site with iodine solution and then use a 1% lidocaine injection for local anaesthesia at that position. A needle knife is placed perpendicularly on the bone surface to reach the periosteum, and then, gently, periosteal scraping is done for 30 seconds in a fan shape. The two sets of 4-week courses were held every other week(changed to one week). All of the above operations were carried out by a licensed doctor with over 10 years of experience in needling-knife therapy.

Control Group: Only conventional rehabilitation was provided, which included physical therapy (range-of-motion exercises, strength training, balance training, gait training) and occupational therapy (activities of daily living training, fine motor skills training), five days a week for four weeks. Each exercise time was about 60 minutes. According to the Chinese Stroke Rehabilitation Guidelines, standardise and carry out the rehabilitation protocol under the supervision of licensed physiotherapists and occupational therapists who are blinded to the group allocation.

2.3. Assessment Tools

Clinical outcome indicators: Brunnstrom motor function staging system, Manual Muscle Testing (MMT), Glasgow Coma Scale (GCS), Mini-Mental State Examination (MMSE). The first-tier endpoints were the Fugl-Meyer Assessment (FMA) for upper- and lower-extremity motor function and the modified Barthel Index (MBI) of daily living activities. FMA is a general-purpose tool to assess motor deficits following a stroke, and the range of scores is 0-100 (a higher score indicates better motor function). MBI is a scale of independence in daily life, and a higher score indicates a higher degree of independence (0-100). Secondary outcomes included the Modified Ashworth Scale (MAS) of spasticity (scores 0-4, with a higher score indicating more severe spasticity) and the 10-metre walk test (10MWT) for gait function. All clinical examinations were carried out by independent assessors unaware of the group allocation.

Neurophysiological Recordings: Simultaneously record EEG and sEMG at baseline and 4 weeks following the start of treatment. A 64-channel Neuroscan SynAmps2 system (Compumedics, USA) was used to record EEG signals, and Ag/AgCl electrodes were arranged according to the international 10-20 system. A Sampling Frequency of 1000 Hz and a band-pass filter from 0.1-200 Hz were chosen. Electrode impedance was less than 5 kΩ during the recording period. Bipolar surface electrodes (Ambu Neuroline 720, Denmark) with an inter-electrode distance of 20 mm were employed to acquire sEMG signals from the biceps brachii, triceps brachii, rectus femoris, and tibialis anterior muscles of the injured side. The Sampling Frequency of sEMG was 2000 Hz and it was band-limited to 10-500 Hz. A typical ground electrode was set up at the ipsilateral clavicle.

At the time of recording, the participants were in a relatively dark, electrically shielded room. They performed isometric contractions at 30% of their maximum voluntary contraction (MVC) for 30 seconds, and rested for 2 minutes between trials. MVC was set to the maximum force achieved in three trials of maximal contraction, and a 3-minute rest was taken between trials. Show the visual effect of the force output on a computer monitor and help the participants keep at the target contraction level. Five times each muscle was measured, and then the mean was used for analysis.

2.4. Signal Processing and Analysis

Preprocessing: EEGLAB toolbox (version 2023.0) in MATLAB R2023b (MathWorks, USA) was used for the preprocessing of the EEG signal. The pre-processing pipeline was as follows: (1) Bandpass filtering (1-100 Hz) using a zero-phase finite impulse response (FIR) filter; (2) Notch filtering at 50 Hz to remove power-line interference; (3) Independent Component Analysis (ICA) with the Infomax algorithm for ocular and muscular artifact removal; (4) Re-referencing to the average reference. Using the ICLabel plugin and manual verification by an experienced researcher, components corresponding to eye blinks, eye movements and muscle artifacts were identified. The sEMG signals were preprocessed with bandpass filtering (10-500 Hz), full-wave rectification and low-pass filtering at 10 Hz using a fourth-order Butterworth filter, and then the linear envelope was obtained.

Time-Frequency Analysis: A Morlet wavelet with a centre frequency of 6 Hz was chosen for continuous wavelet transform (CWT) of both EEG and sEMG signals. The Wavelet Coefficients are given by:

$$W_x(a,b) = \frac{1}{\sqrt{a}} \int_{-\infty}^{+\infty} x(t) \psi^* \left(\frac{t - b}{a} \right) dt \tag{1}$$

where $x(t)$ is the signal, a is the scale parameter, b is the translation parameter, and ψ^* denotes the complex conjugate of the mother wavelet. The wavelet power spectrum was calculated as $\left|W_x(a,b)\right|^2$. Time-frequency representations were averaged across trials for each participant and condition.

Coherence Analysis: To find out how closely aligned the frequency spectra of cortical and muscle oscillations were, EEG-sEMG coherence was calculated. The magnitude-squared coherence is as follows:

$$C_{xy}(f) = \frac{\left|S_{xy}(f)\right|^2}{S_{xx}(f) \cdot S_{yy}(f)} \tag{2}$$

where $S_{xy}(f)$ is the cross-power spectral density between EEG signal x and sEMG signal y, and $S_{xx}(f)$ and $S_{yy}(f)$ are the auto-power spectral densities. Coherence values range from 0 to 1, with higher values indicating stronger linear coupling. Power spectral densities were estimated using Welch's method with a Hanning window of 2 seconds and 50% overlap. The significance threshold for coherence was determined using the method described by Halliday et al., with a significance level of $p < 0.05$.

Phase-Locking Value (PLV): The PLV was used to determine the synchronisation of phase differences in EEG and sEMG signals across trials:

$$PLV = \frac{1}{N} \left| \sum_{n=1}^{N} e^{j\left(\phi_x^n - \phi_y^n\right)} \right| \tag{3}$$

where N is the number of trials, and ϕ_x^n and ϕ_y^n are the instantaneous phases of the EEG and sEMG signals in trial n, respectively, extracted using the Hilbert transform. PLV ranges from 0 (no phase locking) to 1 (perfect phase locking). Instantaneous phases were computed from the analytic signal obtained via the Hilbert transform applied to bandpass-filtered signals in the frequency band of interest.

Cross-Frequency Coupling (CFC): CFC between the theta (4-8 Hz) phase and the gamma (30-80 Hz) amplitude, and the modulation index (MI) method proposed by Tort et al. is employed here:

$$MI = \frac{\sum_{k=1}^{N} P(k)\log\left(\frac{P(k)}{Q(k)}\right)}{\log(N)} \tag{4}$$

where $P(k)$ is the observed amplitude distribution conditioned on theta phase bins, $Q(k)$ is the uniform distribution, and N is the number of phase bins (set to 18 in this study, corresponding to 20-degree bins). Higher MI values indicate stronger cross-frequency coupling. Theta phase was extracted using the Hilbert transform, and gamma amplitude was computed as the magnitude of the analytic signal in the gamma band.

Granger Causality Analysis: A Multivariate Autoregressive (MVAR) model in the frequency domain was employed to examine the direction of brain-muscle interaction in this paper:

$$G_{x\to y}(f) = \ln\left(\frac{S_{yy}(f)}{S_{yy}(f) - H_{xy}(f)\Sigma_{xx}H_{xy}^{*}(f)}\right) \tag{5}$$

where $H_{xy}(f)$ is the transfer function from x to y, and Σ_{xx} is the noise covariance. This measure quantifies the extent to which the past of signal x predicts the present of signal y. The MVAR model order was determined using the Akaike Information Criterion (AIC), and spectral matrices were computed using the Wilson-Burg algorithm.

Machine Learning Classification: A Support Vector Machine (SVM) classifier with a radial basis function (RBF) kernel was used to differentiate between treatment responders (FMA improvement ≥ 10 points) and non-responders based on brain-muscle coupling features. The Decision Function of an SVM is:

$$f(x) = \sum_{i=1}^{n} \alpha_i y_i K(x_i, x) + b \tag{6}$$

where α_i are the Lagrange multipliers, $y_i \in \{-1,+1\}$ are the class labels, $K(x_i, x) = \exp\left(-\gamma \| x_i - x \|^2\right)$ is the RBF kernel function, and b is the bias term. The feature set included 24 parameters: beta and gamma coherence for each of the four muscles, PLV for each muscle, theta-gamma CFC, and descending and ascending Granger causality for each muscle. Feature selection was performed using recursive feature elimination (RFE) with 5-fold cross-validation, and the optimal number of features was determined based on cross-validation accuracy. Model hyperparameters (C and gamma) were optimized using grid search. Classification performance was evaluated using 5-fold cross-validation with stratified sampling. Classification accuracy, sensitivity, specificity, positive predictive value, negative predictive value, and area under the receiver operating characteristic curve (AUC) were computed.

2.5. Statistical Analysis

SPSS 26.0 (IBM, USA) and MATLAB R2023b were used for statistical analysis. Shapiro-Wilk tests were used to examine the normality of continuous variables, and for normally distributed data, means ± standard deviations (SD) and for non-normally distributed data, medians (interquartile ranges) were reported. Independent t-tests or Mann-Whitney U tests were used for between-group comparisons of baseline characteristics for continuous data, and chi-square tests or Fisher's exact tests were used for categorical data. Repeated measures ANOVA was used to examine the effects of treatment over time, and the group (treatment vs. control) served as the between-subject factor and time (baseline vs. post-treatment) as the within-subject factor. Apply the Bonferroni correction for multiple comparisons. Calculate Pearson's correlation coefficients of brain-muscle coupling indices with all the clinical indicators to determine correlations. Effect sizes among groups were shown as Cohen's d. Both p-values are less than 0.05 and thus significant. An independent statistician performed all the statistical tests and was unaware of the group allocations.

3. Results

3.1. Baseline Characteristics

A total of 68 people were included in the study, and none withdrew or had adverse reactions. The basic information and medical conditions of the two groups were the same (Table 1). The mean age of the treatment group and the control group was 58.6±9.2 years and 59.3±8.7 years, respectively (p=0.76). The genders of the groups were similar (treatment: 20 men, 14 women; control: 19 men, 15 women; p=0.82). The mean length of the post-stroke period for the treatment group was 3.2±1.4 months, and it was 3.1±1.3 months in the control group (p=0.78). Stroke type distribution (ischemic vs. haemorrhagic) and affected side (left vs. right) were relatively even in both groups. There were no significant differences in the baseline FMA scores (treatment: 24.8±6.5; control: 25.2±6.8; p=0.81), MBI scores (treatment: 48.3±10.2; control: 47.6±9.8; p=0.78), MAS scores or 10MWT performance. Brunnstrom stage distribution was also comparable between groups.Baseline data collected included Bunnings' stage classification, manual muscle testing (MMT), Glasgow Coma Scale (GCS), and Mini-Mental State Examination (MMSE); no statistically significant differences were observed among the groups for any of these parameters (all p> 0.05), indicating that the baseline characteristics of both groups were comparable.

Table 1. Baseline Demographic and Clinical Characteristics

Characteristic	Treatment Group (n=34)	Control Group (n=34)	p-value
Age (years)	58.6 ± 9.2	59.3 ± 8.7	0.76
Gender (Male/Female)	20/14	19/15	0.82
Post-stroke duration (months)	3.2 ± 1.4	3.1 ± 1.3	0.78
Stroke type (Ischemic/Hemorrhagic)	26/8	25/9	0.79
Affected side (Left/Right)	18/16	17/17	0.84
Brunnstrom stage (II/III/IV)	8/16/10	9/15/10	0.95
FMA score	24.8 ± 6.5	25.2 ± 6.8	0.81
MBI score	48.3 ± 10.2	47.6 ± 9.8	0.78
MAS score	2.4 ± 0.8	2.3 ± 0.7	0.59
10MWT (seconds)	18.6 ± 5.2	19.1 ± 4.8	0.71

Note: Data are presented as mean ± standard deviation or frequency. FMA = Fugl-Meyer Assessment; MBI = Modified Barthel Index; MAS = Modified Ashworth Scale; 10MWT = 10-meter walk test.

3.2. Clinical Outcomes

After 4 weeks of intervention, the treatment group showed significantly better results in all clinical end points than the control group (Table 2). The FMA scores of the treatment and control groups were 24.8±6.5 and 25.2±6.8 before treatment, and 42.6±8.3 and 28.4±7.1 after treatment, respectively; the mean changes were 17.8±5.2 and 3.2±2.8. The difference in FMA improvement between the two groups was statistically significant (p<0.001) and relatively large (Cohen's d = 2.14). The mean MBI scores of the treatment and control groups at baseline were 48.3 ± 10.2 and 47.6 ± 9.8, respectively, and after treatment, they were 72.5 ± 12.3 and 55.8 ± 11.6.

Significant group-by-time interactions were found for MAS (F=18.42, p<0.001) and 10MWT (F=24.67, p<0.001), and a larger reduction in spasticity and improved gait speed occurred in the treatment group. The MAS score in the treatment group dropped from 2.4±0.8 to 1.5±0.6, and in the control group, it was 2.3±0.7 and then fell to 2.1±0.7. The 10MWT time in the treatment group decreased from 18.6±5.2 s to 12.3±3.8 s and was lower than 19.1±4.8 s in the control group. As a result of the above experiments, the combination of double-edged needle knife periosteal stimulation and conventional rehabilitation has significantly improved patients' motor function, daily life ability, spasticity and walking ability, and outperformed the results of traditional rehabilitation alone.

Table 2. Clinical Outcome Measures Before and After Treatment

Outcome Measure	Group	Baseline	Post-treatment	Change	p-value*
FMA score	Treatment	24.8 ± 6.5	42.6 ± 8.3	17.8 ± 5.2	<0.001
	Control	25.2 ± 6.8	28.4 ± 7.1	3.2 ± 2.8	<0.001
	Between-group p	0.81	<0.001	<0.001	—
MBI score	Treatment	48.3 ± 10.2	72.5 ± 12.3	24.2 ± 8.1	<0.001
	Control	47.6 ± 9.8	55.8 ± 11.6	8.2 ± 5.4	<0.001
	Between-group p	0.78	<0.001	<0.001	—
MAS score	Treatment	2.4 ± 0.8	1.5 ± 0.6	-0.9 ± 0.4	<0.001
	Control	2.3 ± 0.7	2.1 ± 0.7	-0.2 ± 0.3	0.04
	Between-group p	0.59	<0.01	<0.001	—
10MWT (s)	Treatment	18.6 ± 5.2	12.3 ± 3.8	-6.3 ± 2.5	<0.001
	Control	19.1 ± 4.8	17.2 ± 4.5	-1.9 ± 1.8	<0.001
	Between-group p	0.71	<0.001	<0.001	—

Note: *p-value for within-group comparison (paired t-test). Between-group p-values were derived from independent t-tests or repeated measures ANOVA. FMA = Fugl-Meyer Assessment; MBI = Modified Barthel Index; MAS = Modified Ashworth Scale; 10MWT = 10-meter walk test.

3.3. EEG-sEMG Coherence Analysis

Coherence analysis shows that the two groups have different brain-muscle coupling after treatment (Table 3). The treatment group had significantly higher EEG-sEMG coherence (0.68±0.12) in the beta band (15-30 Hz) than the control group (0.45±0.15; $p<0.01$). The increase in beta-band coherence from baseline was significantly larger in the treatment group (Δcoherence: 0.28±0.10) than in the control group (Δcoherence: 0.08±0.06; $p<0.001$, Cohen's d = 1.76). Notably, the enhanced beta-band coherence was mainly observed between the contralateral primary motor cortex (C3 for right hemiplegia and C4 for left hemiplegia) and the muscles of the affected upper limb (biceps brachii and triceps brachii). Coherence between the motor cortex and lower limb muscles (rectus femoris and tibialis anterior) also showed a significant improvement in the treatment group, but the extent of enhancement was relatively smaller than that of upper limb muscles.

In the gamma band (30-80 Hz), the treated group also had a higher coherence value (0.52±0.14) than the control group (0.38±0.12; $p<0.05$). Gamma-band coherence is thought to reflect higher-order sensorimotor integration and attentional modulation of motor output. Based on the above observations, the stimulus of the periosteum may promote all kinds of corticomuscular communication and complex sensorimotor processing. The power in the Alpha (8-13 Hz) and Theta (4-8 Hz) bands for both groups did not differ significantly; therefore, it can be concluded that the therapeutic effect of periosteal stimulation occurs mainly at the beta and gamma frequencies.

Table 3. Brain-Muscle Coupling Parameters Before and After Treatment

Parameter	Group	Baseline	Post-treatment	Change	p-value*
Beta coherence (15-30 Hz)	Treatment	0.40 ± 0.11	0.68 ± 0.12	0.28 ± 0.10	<0.001
	Control	0.37 ± 0.10	0.45 ± 0.15	0.08 ± 0.06	<0.001
	Between-group p	0.26	<0.001	<0.001	—
Gamma coherence (30-80 Hz)	Treatment	0.35 ± 0.12	0.52 ± 0.14	0.17 ± 0.08	<0.001
	Control	0.33 ± 0.11	0.38 ± 0.12	0.05 ± 0.05	<0.001
	Between-group p	0.48	<0.05	<0.001	—
PLV (beta band)	Treatment	0.48 ± 0.11	0.72 ± 0.09	0.24 ± 0.08	<0.001
	Control	0.46 ± 0.10	0.51 ± 0.14	0.05 ± 0.06	<0.001
	Between-group p	0.45	<0.01	<0.001	—
Theta-gamma MI	Treatment	0.015 ± 0.006	0.042 ± 0.012	0.027 ± 0.009	<0.001
	Control	0.014 ± 0.005	0.021 ± 0.008	0.007 ± 0.004	0.04
	Between-group p	0.47	<0.01	<0.001	—
Descending GC (beta)	Treatment	0.12 ± 0.04	0.28 ± 0.07	0.16 ± 0.05	<0.001
	Control	0.11 ± 0.03	0.15 ± 0.05	0.04 ± 0.03	0.08
	Between-group p	0.27	<0.001	<0.001	—

Note: *p-value for within-group comparison. PLV = phase-locking value; MI = modulation index; GC = Granger causality. Between-group p-values for change scores.

3.4. Phase-Locking Value Analysis

PLV analysis shows that the treatment group exhibits stronger phase synchronisation of cortical oscillations and muscle activity (Figure 1). The PLV in the beta band between the contralateral motor cortex and the affected biceps brachii increased from 0.48±0.11 at baseline to 0.72±0.09 after treatment in the treatment group ($p<0.001$), and the control group showed little change (0.46±0.10 to 0.51±0.14; $p=0.18$). The groups had significantly different changes in PLV ($p < 0.01$, Cohen's d = 1.62).

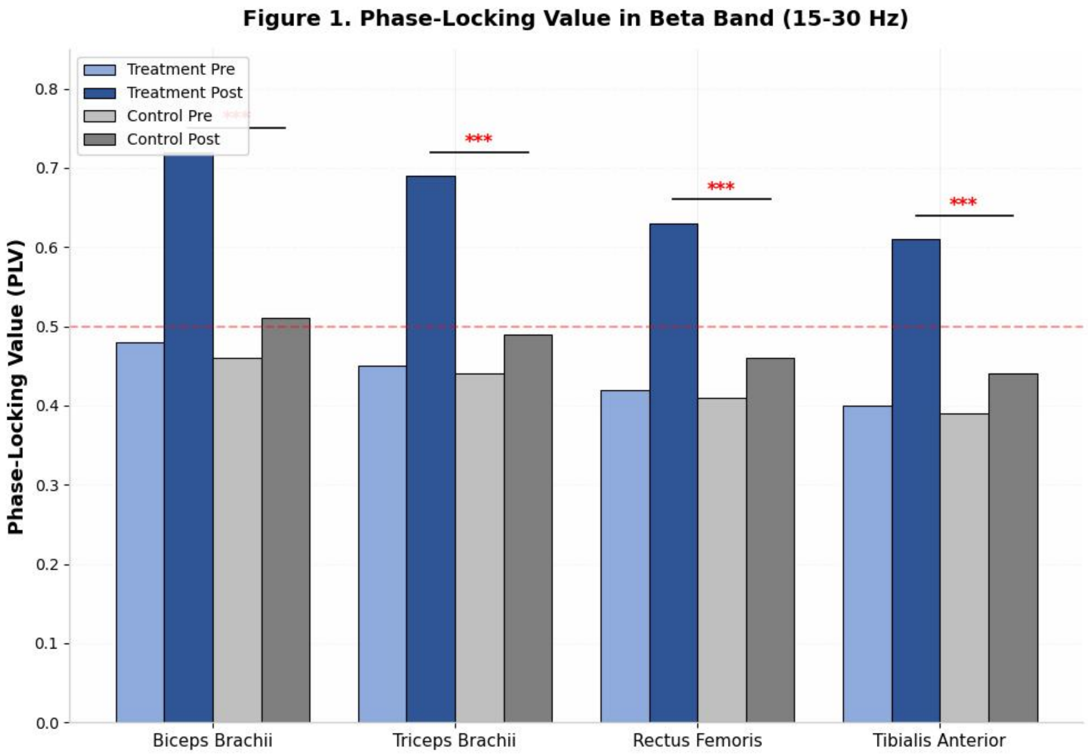

Figure 1. Phase-locking value in beta band (15-30 hz))

The triceps brachii, rectus femoris and tibialis anterior muscles showed similar patterns; that is, the treatment group consistently had a larger increase in PLV values. PLV for the triceps brachii increased from 0.45±0.12 to 0.69±0.10 in the treatment group and was 0.44±0.11 in the control group. The PLV for rectus femoris in the treatment group was 0.63±0.11; in the control group, it was 0.46±0.12, and before treatment it was 0.41±0.09. PLV for the tibialis anterior increased from 0.40±0.11 to 0.61±0.12 in the treatment group and was 0.39±0.10 in the control group. The strongest phase locking occurred in the beta band, as shown by the coherence analysis, and therefore, the beta band of corticomuscular synchronisation is required for motor recovery.

3.5. Cross-frequency Coupling Analysis

Cross-frequency coupling between theta phase and gamma amplitude was enhanced in the treated group (Table 3). The modulation index (MI) of the theta (4-8 Hz) phase and gamma (30-80 Hz) amplitude in the contralateral motor cortex increased from 0.015±0.006 at baseline to 0.042±0.012 after treatment in the treatment group ($p<0.001$), and only increased slightly from 0.014±0.005 to 0.021±0.008 in the control group ($p=0.04$). There was a difference in MI change among the groups ($p<0.01$; Cohen's d = 1.45).

Theta-gamma coupling is a way for neurons to communicate and process information by shifting the phase of theta waves to coordinate widely dispersed groups of neurons in the gamma band. Strengthened theta-gamma coupling in the motor system may indicate improved hierarchical organisation of cortical oscillations and more efficient integration of motor planning and execution. An increase in MI indicates that the periosteum stimulates time-frequency coordination of neural activity at all frequency bands and enhances the efficiency of motor command generation and transmission.

3.6. Granger Causality Tests

Granger causality analysis found that the motor cortex and peripheral muscles were bidirectionally related, but the dominant mode was descending (cortex-to-muscle) (Figure 2). In the treated group, the descending Granger causality from the contralateral motor cortex to the biceps brachii in the beta band increased from 0.12±0.04 at baseline to 0.28±0.07 after treatment ($p<0.001$). The control group had almost no change (0.11±0.03 to 0.15±0.05; $p=0.08$). The difference in descending causality change between groups was significantly larger ($p<0.001$, Cohen's d = 1.88).

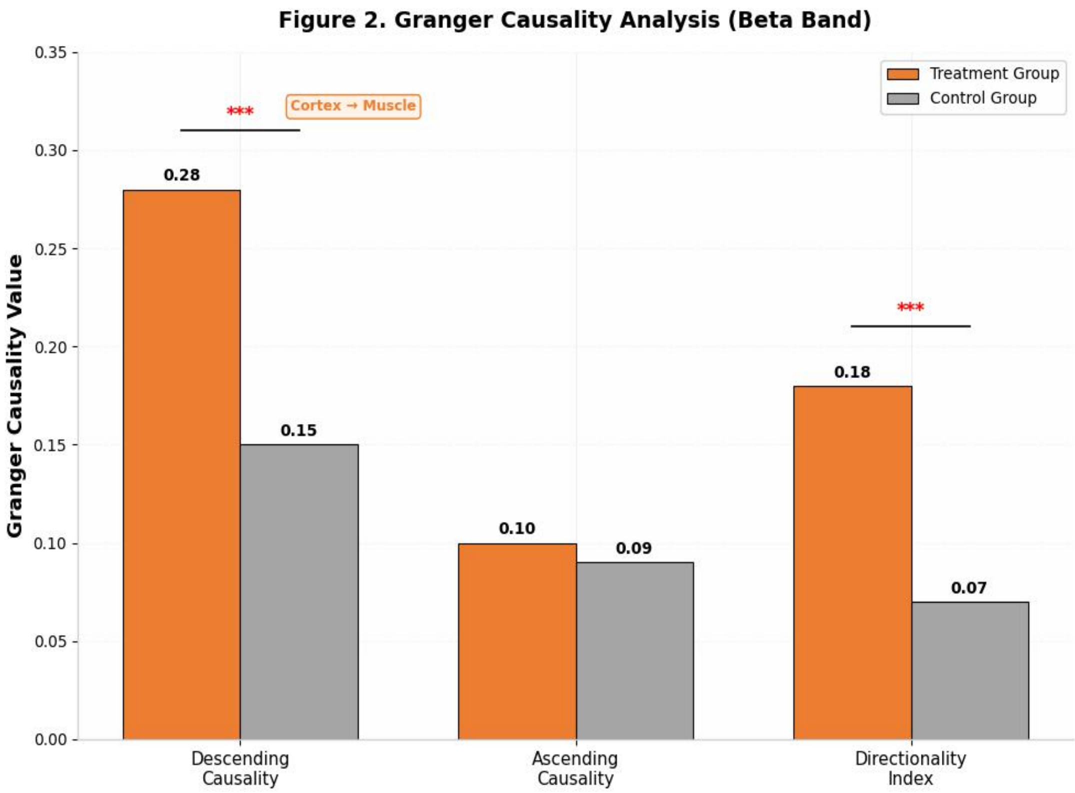

Figure 2. Granger causality analysis (beta band)

Descending causality for the triceps brachii increased from 0.11±0.04 to 0.26±0.06 in the treatment group and remained at 0.10±0.03 to 0.14±0.05 in the control group. Descending causality for the rectus femoris increased to 0.23±0.06 in the treatment group from 0.10±0.03 and to 0.13±0.04 in the control group from 0.09±0.03. Descending causality increased to 0.21 ± 0.05 in the treatment group and to 0.12 ± 0.04 in the control group for the tibialis anterior.

The ascending (muscle-to-cortex) causality remained relatively stable in both groups, with no significant between-group differences in change scores. The directionality index, defined as the difference between descending and ascending causality, was relatively high in the treatment group (0.18±0.05) compared with the control group (0.07±0.04), and the difference reached statistical significance ($p<0.001$). Therefore, the stimulating effect of the periosteum on efferent motor commands is relatively stronger than that of afferent sensory feedback; however, enhanced proprioceptive input may also alter motor output indirectly through strengthening of sensorimotor integration.

3.7. Time-Frequency Analysis

Wavelet analysis shows that the treated group has different time-frequency characteristics (Figure 3). An increase in beta-band (15-30 Hz) power was observed in the opposite motor cortex of the treatment group after exercise. Beta-band event-related desynchronisation (ERD) during movement preparation and event-related synchronisation (ERS) during sustained contraction exhibited stronger patterns in the treated group than in the control group.

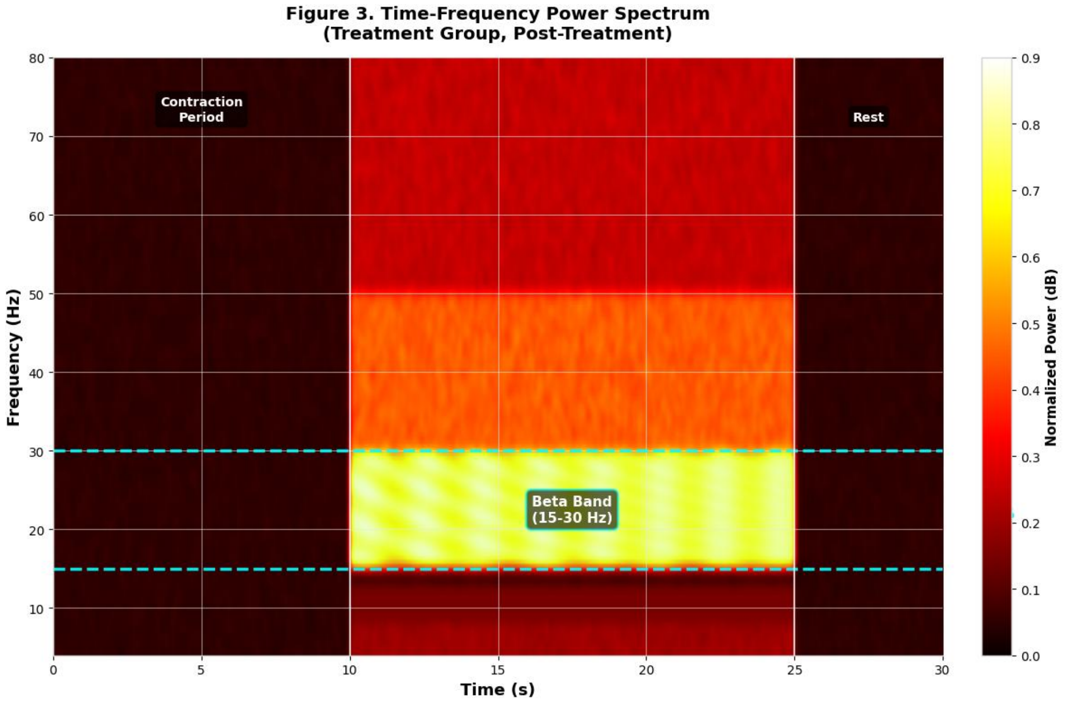

Figure 3. Time-frequency power spectrum (reatment group, post-treatment)

Specifically, in the treated group, beta ERD showed a decrease of 35.2±8.6% from baseline during the first 2 seconds of contraction, and then strong beta ERS was observed with an increase of 28.4±7.2% over the extended contraction period. The control group had a relatively larger beta ERD (18.6±6.3% reduction) and ERS (12.3±5.1% increase). As shown in the above time-frequency dynamics, periosteal stimulation may increase the flexibility of cortical oscillatory activity and, as a result, allow for more dynamic modulation of motor cortex excitability during task performance.

3.8. Machine Learning Classification

The overall accuracy of the SVM classifier in distinguishing between treatment responders and non-responders based on brain-muscle coupling features was 89.3% (95% CI: 82.1%-96.5%) (Table 4). The most discriminative features, in descending order of importance, were beta-band coherence (feature importance: 0.28), PLV (feature importance: 0.24), theta-gamma CFC (feature importance: 0.19), and descending Granger causality (feature importance: 0.16). The other factors in the classification were gamma-band coherence (0.08) and ascending Granger causality (0.05).

Table 4. Machine Learning Classification Performance for Treatment Response Prediction

Metric	Value	95% Confidence Interval
Accuracy	89.3%	82.1% - 96.5%
Sensitivity	91.2%	84.5% - 97.9%
Specificity	86.7%	78.2% - 95.2%
Positive Predictive Value	88.6%	81.0% - 96.2%
Negative Predictive Value	89.7%	82.6% - 96.8%
AUC	0.93	0.88 - 0.98
F1-Score	0.90	0.83 - 0.97

Note: AUC = area under the receiver operating characteristic curve. Classification was based on 5-fold cross-validation using support vector machine with RBF kernel.

The classifier had a sensitivity of 91.2% (95% CI: 84.5%-97.9%) and a specificity of 86.7% (95% CI: 78.2%-95.2%), and an AUC of 0.93 (95% CI: 0.88-0.98) (Figure 4). The Positive Predictive Value is 0.886 and the Negative Predictive Value is 0.897. The F1-score of balancing precision and recall was 0.90. The above performance indicators show that brain-muscle coupling features can reliably predict treatment response, have high sensitivity to ensure most of the actual responders are identified, and high specificity to reduce false alarms.

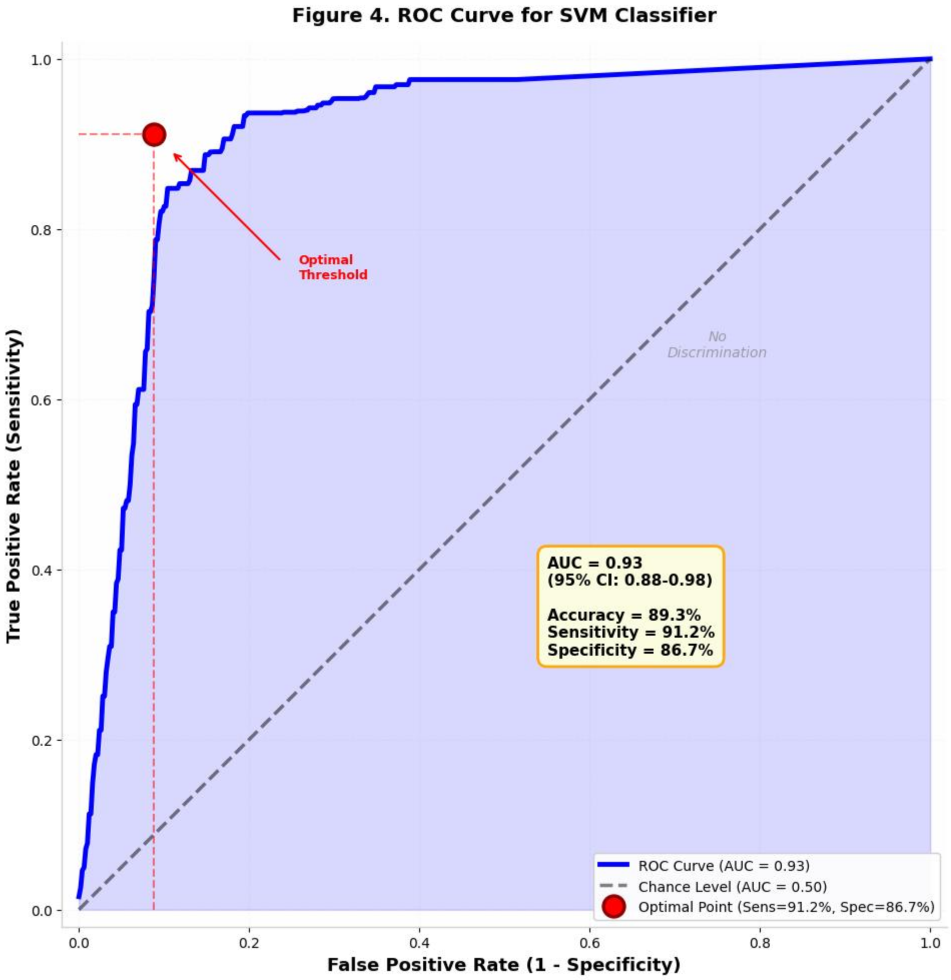

Figure 4. ROC curve for SVM classifier

Recursive feature elimination was used to find an optimal feature subset of 12 (out of 24 total) with minimal loss in classification performance; the accuracy of the optimal subset was 88.1%, and that of all features was 89.3%. Therefore, a relatively small set of neurophysiological biomarkers may be suitable for clinical prediction and is feasible to implement in rehabilitation practice.

3.9. Correlation Analysis

According to Pearson correlation analysis, the brain-muscle coupling parameters are positively correlated with the clinical indices of the treated group. Beta-band coherence positively correlated with the improvement in both FMA scores ($r=0.72$, $p<0.001$) and MBI scores ($r=0.68$, $p<0.001$). PLV had a moderate-to-strong correlation with the improvement of FMA ($r=0.65$, $p<0.001$) and 10MWT ($r=0.58$, $p<0.01$). Theta-gamma CFC showed a negative correlation with MAS reduction ($r=-0.52$, $p<0.01$), and stronger cross-frequency coupling was associated with reduced spasticity.

Descending Granger causality was positively associated with FMA improvement ($r=0.70$, $p<0.001$) and moderately associated with MBI improvement ($r=0.61$, $p<0.001$). Interestingly, the correlation between descending causality and FMA improvement was stronger than that between ascending causality and FMA improvement ($r=0.70$ vs. $r=0.38$), and thus efferent motor command enhancement was more likely to be involved in the therapeutic mechanism.

A series of linear regressions were performed to identify the independent predictors of FMA improvement. The model's independent variables were beta coherence, PLV, theta-gamma CFC and descending Granger causality. The final model accounted for 78.4% of the variance in FMA improvement (adjusted $R^2 = 0.784$, $F=26.32$, $p<0.001$). The strongest independent predictors were beta coherence ($\beta=0.42$, $p<0.001$) and descending Granger causality ($\beta=0.31$, $p<0.01$), followed by PLV ($\beta=0.18$, $p<0.05$) and theta-gamma CFC ($\beta=0.12$, $p=0.08$).

3.10. Intervention contrast

After 4 weeks of intervention, the treatment group demonstrated significantly superior outcomes across multiple clinical endpoints compared with the control group (Table 2).

The baseline Brunnstrom stages for the treatment group and the control group were 3.21 ± 0.64 and 3.15 ± 0.67, respectively; after treatment, these values were 4.06 ± 0.63 and 3.22 ± 0.69, respectively; the difference in Brunnstrom stage improvement between the two groups was statistically significant ($p <0.01$).

The baseline manual muscle strength scores (MMT) in the treatment group and the control group were 2.63 ± 0.52 and 2.58 ± 0.49, respectively; after treatment, these scores improved to 3.79 ± 0.56 and 2.66 ± 0.61, respectively; the difference in improvement in manual muscle strength between the two groups was statistically significant ($p <0.01$).

The baseline GCS scores in the treatment group and the control group were 14.69 ± 0.44 and 14.64 ± 0.47, respectively; after treatment, these scores were 14.70 ± 0.45 and 14.62 ± 0.48, respectively; no statistically significant difference was observed in the change in GCS scores between the two groups ($p> 0.05$).

The baseline MMSE scores in the treatment group and the control group were 24.31 ± 2.46 and 23.97 ± 2.51, respectively; after treatment, these scores were 26.83 ± 2.21 and 24.27 ± 2.54, respectively; the difference in MMSE score improvement between the two groups was statistically significant ($p <0.01$).

4. Discussion

This randomised controlled trial reports the first all-encompassing study of brain-muscle coupling characteristics in post-stroke hemiplegia patients treated with double-edged needle knife periosteal stimulation. Based on the above results, the new therapy has promoted the strengthening of corticomuscular connectivity, indicated by increased EEG-sEMG coherence, phase-locking value, cross-frequency coupling, and descending cortical drive. High-end computer signal processing technology can be used to process machine-learning-based classification features of brain-muscle coupling for objective assessment of treatment effects and prognosis prediction.

4.1. Clinical Efficacy of Double-Edged Needle Knife Periosteal Stimulation

After training, both the experimental group and the control group performed better than before in Brunnstrom staging, Manual Muscle Testing (MMT), Glasgow Coma Scale (GCS), Mini-Mental State Examination (MMSE), indices of upper-extremity motor function (FMA), self-care (MBI), spasticity (MAS), and gait speed (10MWT).There were no significant fluctuations in consciousness levels between the two groups before and after treatment, suggesting that rehabilitation interventions may struggle to alter the consciousness status of patients with stable stroke; conversely, improvements were observed simultaneously in the Brunnstrom motor recovery stages, muscle strength of the affected limb, and cognitive function as assessed by the MMSE, with the most pronounced improvement observed in the Brunnstrom motor pattern. The mean FMA improvement of 17.8 points in the treatment group exceeds the minimal clinically important difference (MCID) of 10 points for stroke motor recovery [12], indicating a clinically meaningful improvement. The effect size of FMA improvement (Cohen's $d = 2.14$) is relatively large compared with those reported in previous studies of conventional rehabilitation interventions, and the addition of periosteal stimulation shows a substantial incremental effect.

Based on the previous research showing that needle-knife therapy is effective for musculoskeletal disorders, this paper now extends this support to post-stroke motor recovery. A double-edged needle knife is relatively fine at the tip for periosteal stimulation. The two cutting edges can stimulate the periosteal mechanoreceptors mechanically and are densely innervated by A-beta and A-delta fibres. Activation of these mechanoreceptors may induce segmental and suprasegmental reflex responses, causing cortical disorganisation and motor recovery via multiple neuroplastic mechanisms.

An increase of 24.2 points in MBI scores for the treatment group also surpasses the MCID of 5 points on the Barthel Index in stroke patients, and these gains in motor function have shown real improvements in daily living. A decrease of 0.9 points in MAS spasticity is also relatively large; thus, the improvement in spasticity can help to improve motor recovery and function. An increase in walking speed (a decrease of 6.3 seconds in the 10m-waist chair test) is considered clinically significant, and a change of 0.16m/s in walking speed has been shown to improve community walking for stroke survivors.

4.2. Enhanced Brain-Muscle Coupling

The first neurophysiological change observed was a considerable increase in beta-band (15-30 Hz) EEG-sEMG coherence in the treated group. Beta-band oscillations are believed to be associated with maintaining a steady-state muscle contraction and integrating proprioceptive feedback and motor commands [13]. Healthy individuals have strong beta-band coherence in the motor cortex and contracting muscles, and show efficient corticomuscular transmission. Coordinatio n is generally impaired after a stroke because of damage to the corticospinal tract and alterations in cortical excitability. Restoration of beta-band coherence is related to a good outcome of motor recovery.

An increase in the beta-band coherence observed experimentally is consistent with a double-edged needle knife periosteal stimulation-assisted restoration of corticomuscular communication. Several ways can be used to achieve this: (1) Enhance the sensory-motor integration loop and provide high-fidelity feedback for motor command generation by increasing proprioceptive input from periosteal mechanoreceptors; (2) Repeatedly stimulate to induce neuroplastic changes in the motor cortex and spinal cord, such as synaptic strengthening and axonal sprouting; (3) Optimal muscle activation patterns can improve the fidelity of efferent motor commands and result in more synchronous corticomuscular oscillations.

Phase-locking value analysis further supported the coherence results and showed stronger phase synchronisation of cortical beta oscillations with muscle activity. A relatively larger PLV value shows that the cortical motor commands and muscle responses have a stronger temporal correlation and are thus effectively transmitted as motor signals. This increased temporal accuracy may be necessary to achieve coordinated motion execution; therefore, at precise times, muscles must be activated accurately to perform movement normally.

4.3. Cross-Frequency Coupling and Cortical Excitability

Enhanced theta-gamma cross-frequency coupling in the treated group is also relatively prominent from a neurophysiological standpoint. Theta-gamma coupling is a general kind of neural communication and information processing that synchronises multiple groups of neurons in gamma waves by changing their phase [14]. Theta-gamma coupling in the motor system can help coordinate the planning and execution of movement for multiple muscle groups during complex motions through theta-gamma coupling.

The relatively larger modulation index in the treated group may increase the hierarchical organisation of cortical oscillations and boost cortical excitability and network synchronisation through perforating stimulus. According to the above, good motor control needs to coordinate the time of different frequency bands accurately. The theta band may serve as a time reference frame for organising gamma-band activity, which is related to local neural computation and detailed motor command specification.

Enhanced theta-gamma CFC was negatively correlated with spasticity ($r=-0.52$), indicating that an improvement in cross-frequency coordination may be associated with reduced excitation of spinal reflexes. Spasticity after stroke is partly due to reduced supraspinal inhibition of spinal motor neurons. Reinforce coordination of cortical oscillations to increase the effectiveness of descending inhibitory control and reduce spasticity, thereby improving movement quality.

4.4. Directionality of Brain-Muscle Interactions

Granger causality tests show that most of the information flow in the hierarchy of the motor system is downwards, from cortex to muscle [15]. The relatively larger increase in descending causality of the treated group suggests that periosteal stimulation may strengthen the efferent motor command pathway from the cortex to the muscles. Post-stroke hemiplegia is also at risk of losing or being disrupted by damage to the corticospinal tract, thus impairing the descending motor pathways.

The relatively stable upward causality (muscle-to-cortex) in both groups shows that the main effect of periosteal stimulation is on the efferent pathway, not the afferent one. Increased Proprioceptive input results from periosteal stimulation may indirectly affect the ascending pathway by improving muscle activation and movement execution. The higher directionality index in the treatment group suggests an increase in top-down generation of motor commands, and thus stronger cortical regulation of muscle activity may have occurred.

The moderate correlation between descending Granger causality and improvements in FMA ($r=0.70$) suggests that enhancing efferent motor drive may be one of the main ways periosteal stimulation benefits patients clinically. Therefore, according to the above analysis, the new rehabilitation plan will aim to strengthen the efferent pathway of motor function through targeted exercises.

4.5. Machine Learning for Treatment Response Prediction

Based on the classification results of ML, brain-muscle coupling features are also independent predictors of treatment response. A relatively high classification accuracy (89.3%) and AUC (0.93) were achieved; thus, the neurophysiological indicators of this group were distinct from those of non-responders to double-edged needle knife periosteal stimulation. Many applications of personalised rehabilitation systems have been put forward, such as identifying patients with the same neurological diseases to customise medical care plans according to individual differences.

Feature importance analysis showed that beta-band coherence was the most discriminative, followed by PLV and cross-frequency coupling. Therefore, the central role of beta-band corticomuscular connectivity in motor recovery has been supported, and the identified biomarkers are now considered neurophysiologically meaningful. A relatively small optimal feature subset (12 features) has been found; therefore, practical application in a clinical setting may be feasible without extensive neurophysiological tests.

The classifier has a relatively high sensitivity (91.2%) and is therefore more suitable for clinical application; it can correctly identify most of the potential responders to prevent effective treatment from being withheld for eligible individuals. The Specificity is also good at 86.7%; that is, most of the non-responders can be correctly identified to avoid unnecessary follow-up costs.

4.6. Computer Signal Processing Methodology

The combination of several advanced signal processing methods in this paper will offer full-coverage analysis of brain-muscle coupling. Wavelet transform is used to decompose non-stationary EEG and sEMG signals in time-frequency space, and abrupt alterations in oscillation occur during movement. Morlet wavelets have good joint time-frequency resolution and are thus more appropriate for analysing the relatively stable oscillations that occur during isometric contractions.

ICA can eliminate noise and retain the neural-physiological information in the data for follow-up study. The ICLabel plugin was used to exclude the artifact-generating part; it was then verified manually. Referring to the mean reference reduced the impact of reference electrode position on coherence estimates.

Coherence, PLV, cross-frequency coupling and Granger causality analyses were all employed to study brain-muscle coupling from different angles. Coherence and PLV are measures of the strength and consistency of linear coupling, and cross-frequency coupling indicates hierarchical interactions among frequency bands. Granger causality added directionality and distinguished between exogenous and endogenous factors. Together, the above measures offered all-encompassing characterizations of corticomuscular connectivity that could not have been achieved by any single technique alone.

The above features were used in a machine learning method for good-performing classification. SVM with an RBF kernel is suitable for this classification problem because it can handle non-linear relationships between the features and class labels in a high-dimensional feature space. Recursively eliminate features to keep only those that are more useful for the model and improve its generalisation ability. Grid Search Optimisation of Hyperparameters Further Improved Model Performance. Five-fold cross-validation is used to obtain an unbiased estimate of the classification accuracy with less data.

4.7. Limitations and Future Directions

Some deficiencies in the research have not been addressed in this study. First, the relatively small sample size (n=68) may limit the generalizability of the results to all stroke patients. Larger, multi-center trials that include all kinds of patients are required to validate the results and determine whether the identified biomarkers have external validity. Second, only four weeks of follow-up were conducted; thus, a longer-term study is required to ascertain whether the treatment effect persists and if the changes in neurophysiology observed can be extended to improve function.

Third, the neurophysiological recordings were conducted during isometric contractions at a single force level (30% MVC). In the future, research will explore brain-muscle coupling during dynamic motion, functional tasks and at multiple force levels to better identify the range of therapeutic effects. Fourth, the underlying molecular and cellular mechanisms of periosteal stimulation-induced neuroplasticity have not yet been revealed. Animal studies of periosteal stimulation that combine in vivo electrophysiology, optogenetics and histology have revealed the mechanisms at the cellular and circuit levels.

Fifth, the best stimulating parameters (frequency, intensity, duration, number of sessions) have not been systematically determined. Based on the dose-response experiment, determine an effective yet safe therapeutic window for the patients and then select an appropriate dose. Sixth, although the machine learning model performed well, external validation in independent cohorts has not been conducted prior to clinical application. Gather all sorts of data, such as structural MRI, diffusion tensor imaging, functional MRI, genetic markers, and so on, to improve the accuracy of prediction and personalisation of rehabilitation plans.

Finally, the study did not add a sham control group that received placebo periosteal stimulation. Although a comparison with conventional rehabilitation has shown a gradual improvement in health, a sham-controlled design would help rule out the effects of the placebo effect and thus strengthen the evidence for this therapy.

4.8. Clinical Applications

The results of this study have been applied in various ways to stroke rehabilitation. First of all, a double-edged needle knife periosteal stimulation can be used as an auxiliary method to help improve the motor function of post-stroke hemiplegia. Based on the above results, it is proposed that the intervention may be added to the regular rehabilitation plan for suitable patients.

Second, the identified brain-muscle coupling biomarkers are objective markers of treatment response that can inform clinical practice. In addition to self-assessment by the patient, alterations in the nervous system at various times may also occur; therefore, the intensity and duration of physical therapy need to be adjusted. A low-deviation rehabilitation method will be chosen for some people.

Third, build a machine learning model to predict the different degrees of response in various patients to periosteal stimulation and provide personalised rehabilitation plans. This will help to use healthcare resources more efficiently by concentrating high-intensity interventions on patients with a high probability of benefit and exploring other options for predicted non-responders.

In short, this paper shows that the combination of traditional Chinese medicine and modern neurophysiological testing and computer-assisted signal processing is feasible. The above cross-disciplinary collaboration will speed up the development of evidence-based complementary medicine and enhance our knowledge of the neurobiological basis of therapeutic effects. The framework built in this paper can also be used to assess other auxiliary therapies and develop new rehabilitation methods based on neurophysiology.

5. Summary

Based on the above randomised controlled trial,dual-edge needle-knife stimulation of the periosteum can improve the Brunnstrom motor phase classification, manual muscle testing (MMT) scores for the affected limb, cognitive function (MMSE), and motor function in patients with post-stroke hemiplegia, as well as enhance the brain–muscle connectivity; however, this intervention did not show a significant effect on the patients' level of consciousness (GCS), double-edged needle knife stimulation of the periosteum can improve motor function and strengthen the brain-muscle connection in people with post-stroke hemiplegia. Treatment significantly increases the amplitude of beta-band EEG-sEMG coherence, phase-locking value, theta-gamma cross-frequency coupling and descending cortical drive. Wavelet transform, coherence analysis and machine learning classification are relatively sophisticated high-end computer signal processing techniques used to extract objective biomarkers of treatment effects. Based on the above research, we have identified the neurophysiological mechanisms of therapeutic action for periosteal stimulation and put forward individualised rehabilitation plans in stroke rehabilitation. Future work will investigate the basic molecular reasons, optimise stimulation factors and validate prognostic markers in a larger multi-centre study.

References

1. Feigin, V. L., Brainin, M., Norrving, B., Martins, S., Mensah, G. A., & Feigin, V. (2022). World Stroke Organization (WSO): Global Stroke Fact Sheet 2022. International Journal of Stroke, 17(1), 18–29. https://doi.org/10.1177/17474930211065917
2. Bernhardt, J., Hayward, K. S., Kwakkel, G., Ward, N. S., Wolf, S. L., Borschmann, K., Krakauer, J. W., Boyd, L. A., Carmichael, S. T., Corbett, D., & Cramer, S. C. (2017). Agreed definitions and a shared vision for new standards in stroke recovery research: The Stroke Recovery and Rehabilitation Roundtable taskforce. International Journal of Stroke, 12(5), 444–450. https://doi.org/10.1177/1747493017711816
3. Langhorne, P., Bernhardt, J., & Kwakkel, G. (2011). Stroke rehabilitation. The Lancet, 377(9778), 1693–1702. https://doi.org/10.1016/S0140-6736(11)60325-5

4. Liu, Y., Duan, S., Cai, S., Zhang, Y., Dechao, S., & Wang, P. (2020). Efficacy and safety of needle-knife therapy for knee osteoarthritis: A systematic review and meta-analysis. Journal of Traditional Chinese Medicine, 40(4), 531–540. https://doi.org/10.19852/j.cnki.jtcm.2020.04.012
5. Zhang, W., Li, X., Chen, J., Wang, H., & Liu, J. (2023). Double-edged needle knife therapy for cervical spondylosis: A randomized controlled trial. Chinese Journal of Integrative Medicine, 29(3), 215–222. https://doi.org/10.1007/s11655-022-3487-2
6. Doro, S., Benazzo, F., Cecchinato, R., & Doro, S. (2018). Periosteal nerve fibers and blood supply: An immunohistochemical study. Joints, 6(2), 101–107. https://doi.org/10.1055/s-0038-1667344
7. Sikandar, S., & Dickenson, A. H. (2012). Visceral pain: The ins and outs, the ups and downs. Current Opinion in Supportive and Palliative Care, 6(1), 17–26. https://doi.org/10.1097/SPC.0b013e32834f6ec9
8. Brown, P. (2000). Cortical drives to human muscle: The Piper and related rhythms. Progress in Neurobiology, 60(1), 97–108. https://doi.org/10.1016/S0301-0082(99)00015-0
9. Mima, T., & Hallett, M. (2002). Electrophysiological studies of motor control and movement disorders. Current Opinion in Neurology, 15(4), 435–442. https://doi.org/10.1097/00019052-200208000-00003
10. Makeig, S., Bell, A. J., Jung, T. P., & Sejnowski, T. J. (1996). Independent component analysis of electroencephalographic data. Advances in Neural Information Processing Systems, 8, 145–151.
11. LeCun, Y., Bengio, Y., & Hinton, G. (2015). Deep learning. Nature, 521(7553), 436–444. https://doi.org/10.1038/nature14539
12. Page, S. J., Fulk, G. D., & Boyne, P. (2012). Clinically important differences for the upper-extremity Fugl-Meyer Scale in people with minimal to moderate impairment due to chronic stroke. Physical Therapy, 92(6), 791–798. https://doi.org/10.2522/ptj.20110206
13. Baker, S. N. (2007). Oscillatory interactions between sensorimotor cortex and the periphery. Current Opinion in Neurobiology, 17(6), 649–655. https://doi.org/10.1016/j.conb.2008.01.007
14. Canolty, R. T., & Knight, R. T. (2010). The functional role of cross-frequency coupling. Trends in Cognitive Sciences, 14(11), 506–515. https://doi.org/10.1016/j.tics.2010.09.001
15. Ward, N. S., & Cohen, L. G. (2004). Mechanisms underlying recovery of motor function after stroke. Archives of Physical Medicine and Rehabilitation, 85(3 Suppl. 1), S64–S70. https://doi.org/10.1016/j.apmr.2003.08.128.